Research Paper

Exosomes Derived From Natural Killer Cells Exert Therapeutic Effect in Melanoma

Liya Zhu, Senthilkumar Kalimuthu, Prakash Gangadaran, Ji Min Oh, Ho Won Lee, Se Hwan Baek, Shin Young Jeong, Sang-Woo Lee, Jaetae Lee, and Byeong-Cheol Ahn✉

Department of Nuclear Medicine, Kyungpook National University School of Medicine and Hospital, Daegu 700-721, Republic of Korea.

✉ Corresponding author: Byeong-Cheol Ahn, MD, PhD, Professor and Director, Department of Nuclear Medicine, Kyungpook National University School of Medicine and Hospital, 50, Samduk 2-ga, Jung Gu, Daegu 700-721, Republic of Korea Tel: 82-53-420-5583 Fax: 82-53-422-0864 E-mail: abc2000@knu.ac.kr

Abstract

Objective: Exosomes are nanovesicles that are released from normal and tumor cells and are detectable in cell culture supernatant and human biological fluids. Although previous studies have explored exosomes released from cancer cells, little is understood regarding the functions of exosomes released by normal cells. Natural killer (NK) cells display rapid immunity to metastatic or hematological malignancies, and efforts have been undertaken to clinically exploit the antitumor properties of NK cells. However, the characteristics and functions of exosomes derived from NK cells remain unknown. In this study, we explored NK cell-derived exosome-mediated antitumor effects against aggressive melanoma *in vitro* and *in vivo*.

Methods: B16F10 cells were transfected with enhanced firefly luciferase (effluc) and thy1.1 genes, and thy1.1-positive cells were immunoselected using microbeads. The resulting B16F10/effluc cells were characterized using reverse transcriptase polymerase chain reaction (RT-PCR), western blotting, and luciferase activity assays. Exosomes derived from NK-92MI cells (NK-92 Exo) were isolated by ultracentrifugation and density gradient ultracentrifugation. NK-92 Exo were characterized by transmission electron microscopy and western blotting. We also performed an enzyme-linked immunosorbent assay to measure cytokines retained in NK-92 Exo cells. The *in vitro* cytotoxicity of NK-92 Exo against the cancer cells was determined using a bioluminescence imaging system (BLI) and CCK-8 assays. To investigate the possible side effects of NK-92 Exo on healthy cells, we also performed the BLI and CCK-8 assays using the human kidney Phoenix™-Ampho cell line. Flow cytometry and western blotting confirmed that NK-92 Exo induced apoptosis in the B16F10/effluc cells. *In vivo*, we used a B16F10/effluc cell xenograft model to detect the immunotherapeutic effect of NK-92 Exo. We injected NK-92 Exo into tumors, and tumor growth progression was monitored using the IVIS Lumina imaging system and ultrasound imaging. Tumor mass was monitored after *in vivo* experiments.

Results: RT-PCR and western blotting confirmed effluc gene expression and protein levels in B16F10/effluc cells. B16F10/effluc activity was found to increase with increasing cell numbers, using BLI assay. For NK-92 Exo characterization, western blotting was performed on both ultracentrifuged and density gradient-isolated exosomes. The results confirmed that NK cell-derived exosomes express two typical exosome proteins, namely CD63 and ALIX. We demonstrated by western blot analysis that NK-92 Exo presented two functional NK proteins, namely perforin and FasL. Moreover, we confirmed the membrane expression of FasL. The enzyme-linked immunosorbent assay results indicated that NK-92 Exo can secrete tumor necrosis factor (TNF)-α, which affected the cell proliferation signaling pathway. The antitumor effect of NK-92 Exo against B16F10/effluc cells *in vitro* was confirmed by BLI (*p* < 0.001) and CCK-8 assays (*p* < 0.001). Furthermore, in normal healthy cells, even after 24 h of co-culture, NK-92 Exo did not exhibit significant side effects. In the *in vivo* experiments, tumors in the vehicle control group were significantly increased, compared with those in the NK-92 Exo-treated group (*p* < 0.05).

Conclusion: The results of the current study suggest that exosomes derived from NK cells exert cytotoxic effects on melanoma cells and thus warrant further development as a potential immunotherapeutic strategy for cancer.

Introduction

Melanoma, the most frequent and malignant primary skin tumor, has a poor prognosis, with a median overall survival of 8–10 months and a 5-year survival rate of 20% [1]. Even with early diagnosis, melanoma still exhibits a poor prognosis because of its rapid proliferation, and therapy remains challenging for physicians. Aggressive metastatic melanoma is generally resistant to multimodal treatment, including surgical resection, chemotherapy, and radiation therapy [2]. Recently, an improved knowledge of the role of the immune system in tumor control has provided new therapeutic approaches to treat advanced melanoma [3].

Natural killer (NK) cells are innate lymphoid cells that play a central role in the immune response against cancer [4]. Two main cytotoxic pathways are necessary for defense against cancer cells. The first involves cytoplasmic granule toxins, predominantly the membrane-disrupting protein perforin, that cooperate with a family of structurally related serine proteases (granzymes). The second pathway involves target-cell death receptors, including Fas, via their cognate ligand, FasL, which induces caspase-dependent apoptosis. Furthermore, NK cells have displayed excellent success in the treatment of metastatic breast cancer or hematological cancers such as acute myeloid leukemia [5, 6]. However, melanomas frequently escape immunotherapy by down-regulating major histocompatibility complex (MHC) class I molecules and inhibiting NKp30, NKp44, and NKG2D expression by NK cells, which impairs their inherent cytolytic activities [7, 8].

Exosomes carry membranous and cytoplasmic constituents of their parental cells, and have been described as a novel means of intercellular interaction to produce various biological effects, including signal transduction, coagulation, disease resistance, and even tumor immune escape [9-11]. The generation of exosomes in peripheral blood mononuclear cells (PBMCs) is thought to be associated with immune surveillance [12]. Exosomes derived from dendritic cells (DCs), the most significant antigen-presenting cells, showed a potent immune activation capability and have been applied in the treatment of tumors [13, 14]. Exosomes derived from mesenchymal stem cells also demonstrated antitumor effects by inhibiting MAP kinase pathways [15]. Although NK cells play an important role in both specific and non-specific immunity, the function of exosomes derived from NK cells has not yet been fully studied or understood [16-18]. To our knowledge, there have been no reports demonstrating an *in vivo* anti-tumor effect of NK-derived exosomes.

In the current study, we isolated exosomes from NK cells and evaluated their potential therapeutic effects against aggressive melanoma cells both *in vitro* and *in vivo*.

Materials and Methods

Cell lines

Mouse melanoma B16F10 cells and the human kidney cell line Phoenix™-Ampho (phoenix-A) were obtained from the American Type Culture Collection (ATCC, Manassas, VA, USA), and cultured in Dulbecco's modified Eagle's medium (Gibco, Rockville, MD, USA) with 10% fetal bovine serum (Gibco) and 1% penicillin-streptomycin (Hyclone, Logan, UT, USA). The human NK cell line, NK92-MI, which was also obtained from the ATCC, was incubated in stem cell growth medium (Cellgro, Freiburg, Germany) supplemented with 2% exosome-depleted human serum and 1% penicillin-streptomycin. A human gastric carcinoma cell line, SNU484, and a human colon cancer cell line, HCT-5, were also used. All cells were cultured at 37 °C in a humidified 5% CO_2 atmosphere.

Transfection of the enhanced firefly luciferase (effluc) gene into B16F10 cells

B16F10 cells were transfected with a recombinant retrovirus containing a plasmid encoding both enhanced firefly luciferase (effluc) and thy1.1 (CD90.1), driven by a long terminal repeat promoter (Retro-LTR-effluc-thy1.1). B16F10 cells expressing both effluc and thy1.1 (CD90.1) were sorted by magnetic cell sorting (Miltenyi Biotec, Auburn, CA, USA). Cells were resuspended in 0.1% bovine serum albumin in phosphate-buffered saline (PBS) and labeled with an anti-CD90.1 antibody (Miltenyi Biotec). After selecting thy1.1 (CD90.1)-positive cells, RT-PCR and western blotting were used to confirm the expression of effluc at the mRNA and protein levels, respectively. The established stable cell line expressing both the effluc and thy1.1 (CD90.1) genes is herein referred to as B16F10/effluc.

Luciferase activity in B16F10/effluc cells

B16F10 and B16F10/effluc cells were seeded at various cell densities in black, clear-bottomed 96-well plates. After 24 h, 3 μl (3 mg/mL) ᴅ-luciferin was added to each well, and effluc activity was measured using an IVIS® Lumina III imaging system (PerkinElmer, Waltham, MA, USA).

Exosome isolation

To obtain NK-92 Exo, NK-92MI cells were cultured in stem cell growth medium for 3 days. The collected supernatant was centrifuged at increasing

speeds to isolate pure NK-92 Exo: 1,500 × g for 3 min, 2,000 × g for 15 min, and 3,000 × g at 4 °C for 20 min to sediment cells and debris. The supernatant was then passed through a 0.22 μm filter and centrifuged at 100,000 × g for 1 h to pellet exosomes using clear ultracentrifuge tubes (Beckman Coulter, Brea, CA, USA) [19]. To confirm the successful isolation of the NK-92 Exo, density gradient ultracentrifugation was also performed. Briefly, exosomes were resuspended in particle-free PBS and purified by ultracentrifugation through 20 and 60% iodixanol (OptiPrep™, Sigma-Aldrich, St Louis, MO, USA); then, the exosomes were collected and washed several times with PBS. The exosome fraction was resuspended in PBS, frozen in liquid nitrogen, stored at −80 °C, and used within 1 week. The protein content of the NK-92 Exo was determined using a bicinchoninic acid protein assay kit (Pierce, Appleton, WI, USA). To confirm the successful isolation of exosomes, western blotting was performed to detect exosome marker proteins. For exosomes isolated by density gradient ultracentrifugation, the following antibodies were used: CD63, ALIX, GM-130, and β-actin. Furthermore, the abundance of functional proteins (FasL and perforin) of the NK cells were measured in NK-92 Exo. For FasL, the membrane protein component was harvested using the Mem-PER™ Plus Membrane Protein Extraction Kit (Thermo Fisher Scientific, Waltham, MA, USA) and detected by western blotting.

Transmission Electron Microscopy (TEM)

TEM was performed to verify the presence of purified exosomes. Ten microliters of exosome suspension was fixed in 2% paraformaldehyde. Formvar/carbon-coated EM grids were placed on top of the exosome suspension, covered, and allowed to adsorb for 20 min in a dry environment. Next, the grids were placed directly onto a drop of 2% uranyl acetate and incubated for 5 min. They were then washed seven times with distilled water for 1 min each and examined using an HT 7700 transmission electron microscope (Hitachi, Tokyo, Japan) operated at 100 kV.

Cellular uptake assay

A cellular uptake assay was performed using a modified chemical protocol [20]. The fluorescent dye DiD (D307, D7757) (5 μM; Invitrogen, Carlsbad, CA, USA) was added to NK-92 Exo suspensions and incubated for 20 min at 37 °C. Samples were washed twice with PBS by ultracentrifugation at 100,000 × g for 1 h, supernatants were removed, and the pellets were resuspended in 60 μl PBS. Aliquots (10 μl) of DiD-labeled and unlabeled NK-92 Exo were placed in clear E-tubes and examined using the IVIS® Lumina III imaging system. Once successful labeling had been confirmed, the DiD-labeled NK-92 Exo were incubated with B16F10/effluc cells for 3, 6, and 12 h at 37 °C. After each incubation period, cells were washed twice with PBS and fixed in 4% paraformaldehyde for 10 min. The samples were covered with VECTASHIELD® mounting medium containing DAPI (Vector Laboratories, Burlingame, CA, USA) after several PBS washes and observed by confocal laser microscopy (LSM 5 Exciter, Carl Zeiss, Oberkochen, Germany).

Cytotoxicity assay

To evaluate NK-92 Exo cytotoxicity against melanoma cells, B16F10/effluc cells were cultured in serum-free medium with different quantities of NK-92 Exo (5 and 20 μg) in black, clear-bottomed 96-well plates for 4, 10, and 24 h. Bioluminescent signals were measured using the IVIS® Lumina III imaging system. To confirm the results obtained by BLI, B16F10/effluc cells were seeded in clear-bottomed 96-well plates for 4, 10, and 24 h, and a standard metabolism-based apoptotic assay, the CCK-8 assay, was performed. FasL triggers the extrinsic apoptotic pathway, leading to the antitumor effect of NK cells. To identify the cell death pathway induced by the presence of FasL in NK-92 Exo, we performed an inhibition assay and assessed cytotoxicity in the B16F10/effluc cells. The B16F10/effluc cells were pre-incubated with 0.25 μg/100 μl FasL inhibitor (AF-016, Kamiya Biomedical Company, USA) for 2 h at 37 °C and then co-incubated with 20 μg NK-92 Exo for 24 h. Cells were then analyzed using BLI and the Cell Counting Kit-8 (Dojindo Molecular Technologies, Rockville, MD, USA). The cytotoxicity assessment was also performed for the human HCC cell line, SNU484/effluc, and the human colon cancer cell line, HCT-5/Rluc. To measure the side effects induced by NK-92 Exo, the cytotoxicity of the NK-92 Exo against normal cells was also determined. Phoenix-A/effluc cells were seeded in 96-well plates, and after co-culture with NK-92 Exo, BLI and CCK-8 were measured in a time-and dose-dependent manner.

Quantification of apoptosis by flow cytometry

To confirm the cytotoxic effects of NK-92 Exo on melanoma cells, Annexin V-fluorescein isothiocyanate (FITC)/propidium iodide (PI) double staining was performed with an Annexin V-FITC Kit (BD Biosciences, San Jose, CA, USA), using a previously reported protocol [15]. B16F10/effluc cells were preincubated with NK-92 Exo for 24 h, harvested, and washed twice with PBS. Then, the samples were

centrifuged and the supernatants were decanted. Cells were resuspended in binding buffer at a concentration of 1×10^6 cells/mL. The stains were added and gently mixed with the cells, which were then incubated for 15 min at room temperature in the dark. Binding buffer (400 µl) was added to each tube before analysis by flow cytometry (FACSCalibur™, BD Biosciences)

Western blot analysis

For a preliminary exploration of the cell death pathway induced by NK-92 Exo, we performed western blot analyses. After treatment with NK-92 Exo for 24 h, cells were harvested and suspended in radioimmunoprecipitation assay buffer (Thermo Fisher Scientific). Extracts were incubated on ice for 30 min and centrifuged at $13,200 \times g$ for 20 min at 4 °C. After centrifugation, supernatants were collected and protein concentrations were determined using a bicinchoninic acid protein assay kit. Whole cell lysates were resolved by sodium dodecyl sulfate polyacrylamide gel electrophoresis and transferred to polyvinylidene fluoride membranes (Millipore, Bedford, MA, USA). Membranes were probed with specific primary antibodies and then with peroxidase-conjugated secondary antibodies. Bands were visualized with an enhanced chemiluminescence kit (Amersham, Arlington Heights, IL, USA). Antibodies against the following proteins were used: caspase-3, cleaved caspase-3, cleaved PARP, cytochrome-c, p-ERK, ERK, p38, and β-actin.

Enzyme-linked immunosorbent assay (ELISA)

NK cells (1×10^6) were seeded in 75-cm^2 flasks with serum-free medium for 2 days; then, the medium was transferred to a centrifuge tube and centrifuged at $1,500 \times g$ for 10 min at 4 °C. Complete extraction buffer (0.5 mL) was added to the NK cells and NK-92 Exo and incubated on ice for 30 min. Finally, the samples were centrifuged at $13,000 \times g$ for 10 min at 4 °C and the supernatant was collected. The concentrations of TNF-α in the samples (NK, NK-92 Exo, and NK medium) were determined using an ELISA kit (Bender MedSystems Diagnostics, Vienna, Austria). Assays were performed in triplicate.

In vivo animal experiment

Pathogen-free 6-week-old female C57BL/6 mice were obtained from SLC Inc. (Shizuoka, Japan). All animal experimental protocols were approved by the Committee for the Handling and Use of Animals at Kyungpook National University. An *in vivo* imaging study was performed on mice (n = 12) using the following procedures: B16F10/effluc cells (1×10^5 cells/100 µl) were subcutaneously injected into the right thighs of C57BL/6 mice. After tumor cell implantation, BLI was performed. After 7 days, NK-92 Exo (20 µg/100 µL PBS) or PBS was injected into the tumors for 2 days. After injection, BLI was performed over 5 days. Regions of interest were drawn manually over the tumor xenografts, and the bioluminescent signal intensity was measured and expressed as photon flux (photons/s).

Immediately following the BLI analysis, three-dimensional (3-D) ultrasound imaging data were collected for each tumor xenograft with a Prospect 3.0 ultrasound micro imaging system (S-Sharp Corporation, New Taipei City, Taiwan). Water-soluble hypoallergenic gel was applied to the location of the xenograft, which was centered in the ultrasound imaging plane. B-mode data were acquired by the automated translation of the 40-MHz probe along the entire length of the orthotropic xenograft. For the analysis of ultrasound data, images were imported to an s-sharp 3-D model for volumetric analysis.

Ex vivo imaging

After all *in vivo* experiments were completed, the mice were sacrificed and the tumors were harvested. The mass of each tumor was measured. For *ex vivo* imaging, the excised tumors were placed on an imaging plate, and images were acquired with the IVIS® Lumina III imaging system.

Statistical Analysis

All numerical data were expressed as the mean ± standard deviation. Inter-group differences were assessed using a two-tailed Student's t-test. p-values < 0.05 were considered statistically significant.

Results

Establishment of B16F10/effluc cells

After seeding the cells in 96-well plates at different densities, the bioluminescence signal was assessed. The B16F10/effluc cells showed a cell number-dependent increase in the bioluminescence signal and there was a strong correlation between cell number and the bioluminescence signal (Supplementary Figs. 1A and B) (R^2 = 0.90). The expression of effluc in the B16F10/effluc cells was confirmed by RT-PCR and western blot analysis (Supplementary Figs. 1C and D).

Characterization of NK-92 Exo

With the goal of evaluating the purity of the exosomes produced, the cell culture supernatant was subjected to sequential low-speed and high-speed centrifugation steps. The NK-92 Exo were examined by TEM, which revealed that the exosomes were

100–150-nm spherical particles with a complete membrane structure, fitting the recognized characteristics of exosomes (Fig. 1A). Further characterization of NK-92 Exo by western blot analysis confirmed the presence of two typical exosomal proteins, namely CD63 and ALIX, and showed that contaminating cellular proteins (GM130 and β-actin) had been eliminated (Fig. 1B). Collectively, these results indicated the successful isolation of NK-92 Exo from the culture medium.

Analysis of Fas ligand and perforin expression in NK-92 Exo

NK cells are known to exert their cytotoxic activity through the release of cytotoxic effectors contained in lytic granules. At the same time, several transmembrane proteins, such as FasL, are exposed on the cell surface and dictate the fates of effector and target cells. Thus, we first established the presence of FasL and perforin in NK-92 Exo by western blot analysis using ultracentrifugation and density gradient isolation methods. The results revealed the presence of FasL, with the typical molecular mass of 42 kDa, in NK-92 Exo. Perforin protein was also detected in the NK-92 Exo lysates (Fig. 2A). Furthermore, in the quantitative assay, the levels of these two proteins were higher in NK-92 Exo compared to that in NK cells (Figs. 2C and D) ($p < 0.05$). To confirm the membrane expression of FasL, the cell envelope of the NK-92 Exo was collected using a membrane protein extraction kit (Mem-PER™ Plus Kit [Thermo Fisher Scientific]) and western blotting was performed (Fig. 2B).
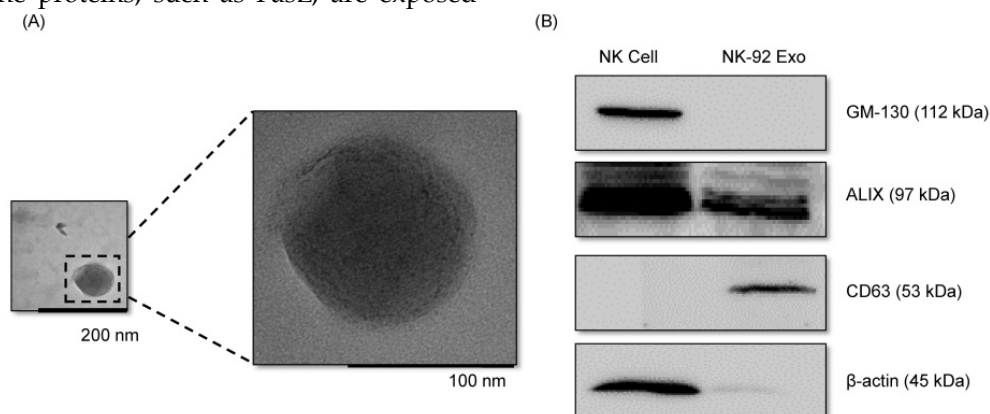

Fig 1. Verification of successful isolation of exosomes. Transmission electron microscopy and western blotting were used to evaluate the phenotype of exosomes recovered from supernatant of NK-92MI cells after culturing them for 3 d. (A) The morphology of exosomes in the recovered pellet was analyzed by transmission electron microscopy (scale bar, 200 nm). (B) The expression of exosome markers (CD63 and ALIX) and negative markers (GM130 and β-actin) was confirmed by western blotting.
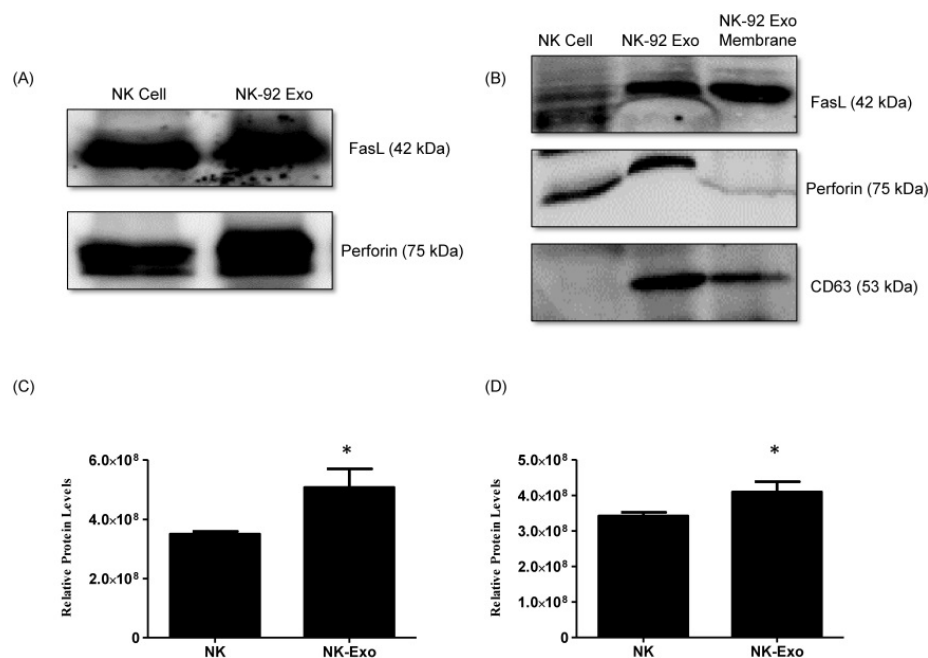

Fig 2. Identification of apoptosis-inducing proteins in NK and NK-92 Exo. Fifty micrograms of total proteins from NK cell and NK-92 Exo lysates were loaded into each lane (*n* = 3). (A) and (B) The apoptosis-inducing proteins FasL and perforin were expressed in both NK cell and NK-92 Exo lysates. FasL was also detected in a membrane proteins enriched extract of NK-92 Exo. (C) and (D) The abundances of FasL and perforin in NK and NK-92 Exo were estimated using the software EvolutionCapt. NK-92 Exo lysates contained higher abundances of FasL and perforin than the NK cell lysates did. Experiments were performed at least in triplicate and values ± SD were plotted. *$p < 0.05$.

(A)   (B)   (C)

4 h   10 h   24 h
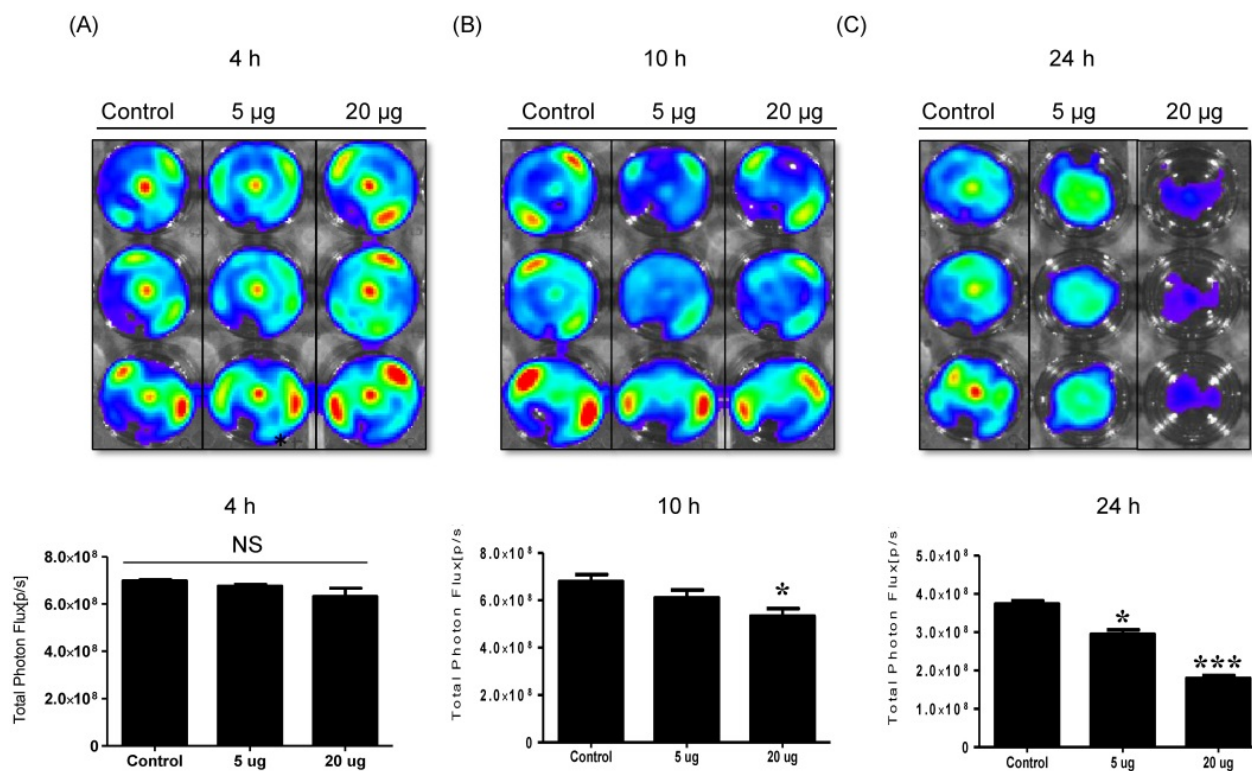

4 h   10 h   24 h

Fig 3. NK cell-derived exosome cytotoxicity against melanoma cells. B16F10/enhanced firefly luciferase (effluc) melanoma cells were co-cultured with two concentrations of NK-92 Exo (5 and 20 µg) and bioluminescence signals were measured at various time points (4, 10, and 24 h). The viability of B16F10/effluc cells decreased at 10 h and 24 h after the co-incubation. Experiments were performed at least in triplicate and values ± SD were plotted. *$p < 0.05$, ***$p < 0.001$.

(A)

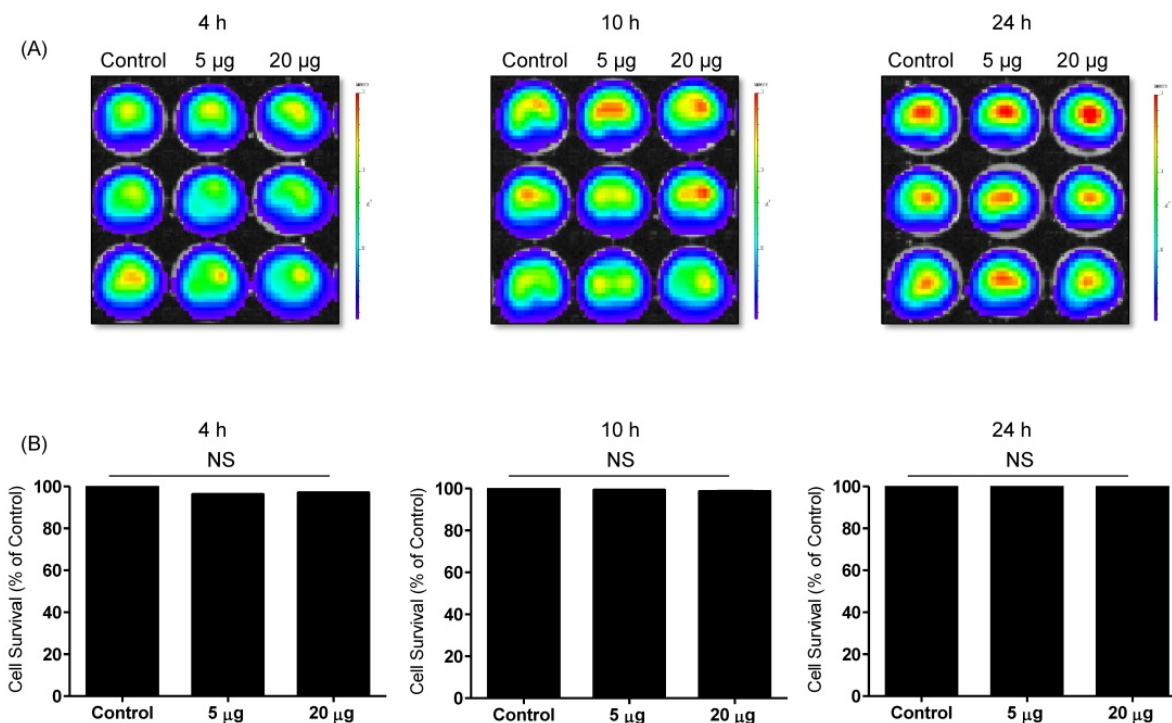4 h   10 h   24 h

(B)

4 h   10 h   24 h

Fig 4. Effects of NK-92 Exo on the proliferation of normal cells. Phoenix-A cells, which are normal human kidney cells, were co-cultured with two concentrations of NK-92 Exo (5 and 20 µg) and bioluminescence signals were measured at 4, 10, and 24 h. NK-92 Exo showed no significant cytotoxicity against the phoenix-A cells even after 24 h (A). To confirm the bioluminescent imaging (BLI) results, a CCK-8 assay was also performed, and the results were consistent with those of BLI (B). Experiments were performed at least in triplicate and values ± SD were plotted.

Cytotoxicity of NK-92 Exo against melanoma cells and side effects of NK-92 Exo

To detect the cytotoxic effect of NK-92 Exo on melanoma cells, we co-cultured different doses of NK-92 Exo with B16F10/effluc cells and performed BLI and CCK-8 assays. The cytotoxicity of NK-92 Exo against the target cells exhibited a time- and dose-dependent effect; the BLI signal strength of the target cells decreased with an increasing concentration and incubation duration (Fig. 3). Moreover, the CCK-8 assay confirmed the results of BLI (Supplementary Fig. 3A). To compare the anti-tumor effects of NK-92 Exo with those of the NK cells, the same method was used to determine the anti-tumor effects of the NK cells, and the results were consistent with the trend shown by NK-92 Exo (Supplementary Figs. 2 and 3B). From the CCK-8 assay, the cell proliferation of the melanoma cells treated with the NK-92-Exo was lower than that of cells treated with NK cells. To measure the side effects of the NK-92 Exo, normal human phoenix-A cells were co-cultured with different doses of NK-92 Exo. The results of both the CCK-8 assay and BLI revealed no significant cytotoxicity of the NK-92 Exo against the normal cells even after co-incubation for 24 h (Fig. 4).

To explore the predominant cell death-mediated pathway triggered by FasL in NK-92 Exo, we assessed the effects of a FasL inhibitor on the cytotoxicity of NK-92 Exo using BLI and CCK-8 assays. The intensity of the bioluminescence signal from the samples without FasL inhibitor (AF-016) was significantly decreased compared with that of the AF-016-containing samples ($p < 0.001$). Furthermore, the samples containing FasL inhibitor also displayed a significantly reduced activity compared with the control group ($p < 0.01$, Figs. 5A and B). The CCK-8 assay displayed similar trends to the BLI analysis; the NK-92 Exo caused the death of 39% of the cancer cells ($p < 0.001$), and the NK-92 Exo with added FasL inhibitor induced the death of 15% of the cells ($p < 0.05$) (Fig. 5C). These results confirmed that NK-92 Exo-mediated cell death is partly related to the presence of FasL.

Cytotoxicity of NK-92 Exo against other cancer cells

To confirm the antitumor effect of NK-92 Exo on other human cancer cells, we selected gastric carcinoma (SNU484/effluc) and colon cancer cells (HCT-15/Rluc). These cells also showed a decreased intensity of the bioluminescence signal after 24 h co-incubation with 20 μg NK-92 Exo (SNU484/effluc: $p < 0.01$, HCT-15/Rluc: $p < 0.001$) (Supplementary Figure 6). These results confirmed that NK-92 Exo might also be useful as a therapy for other cancer types.

Tumor cell uptake of NK-92 Exo

To explore the internalization of NK-92 Exo, B16F10/effluc cells were treated with DiD-labeled NK-92 Exo for 3, 6, and 12 h. Confocal laser microscopy imaging detected the labeled NK-92 Exo (red staining) in the cancer cells in a time-dependent manner (Fig. 6).
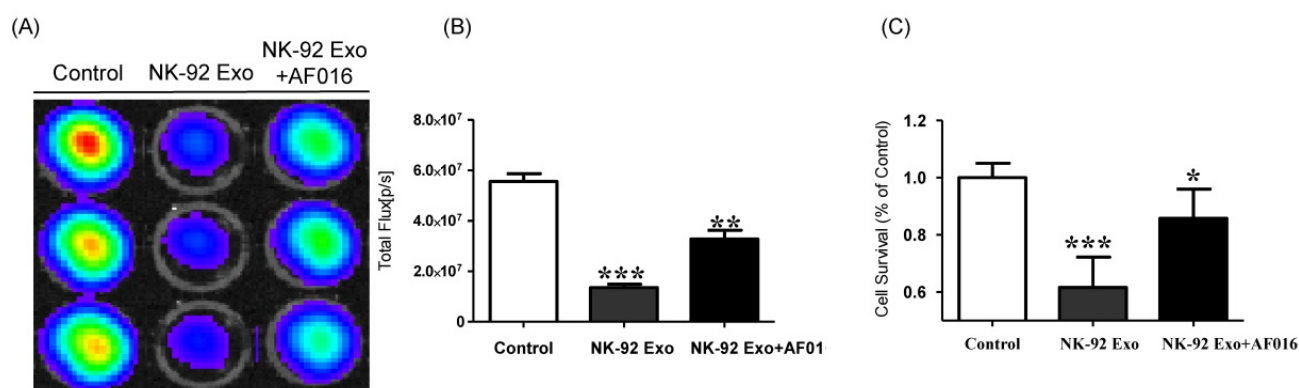

Fig 5. Detection of cytotoxic activity of NK-92 Exo. (A) The cytotoxic effects of NK-92 Exo on B16F10/effluc cells were inhibited by a FasL inhibitor (AF016). (B) Quantitation of the cytotoxic effect. (C) The results of the CCK-8 assay were consistent with those of the BLI assay. Experiments were performed in triplicate and mean values ± SD were plotted. *p <0.05, **p <0.01, ***p <0.001.
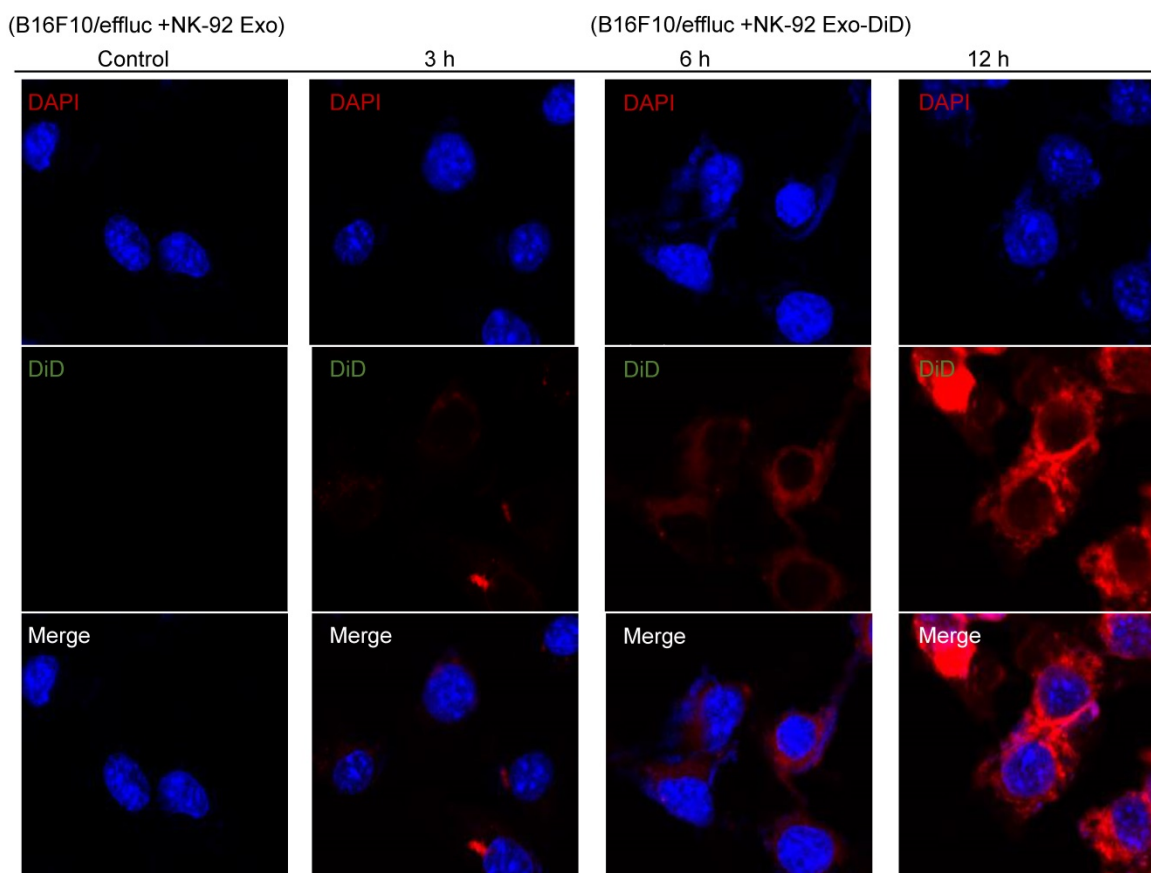
Fig 6. Interaction of NK-92 Exo with melanoma cells. The B16F10/effluc cells were co-incubated with vehicle, NK-92 Exo, and fluorescent dye (DiD)-labeled NK-92 Exo (10 µg). Confocal microscopy images were obtained after 3, 6, and 12 h co-incubation.

Effects of NK-92 Exo on B16F10/effluc cell apoptosis

To explore the induction of apoptosis by NK-92 Exo, we stained NK-92 Exo-treated cells with Annexin V-FITC. After successful staining, the cells were analyzed by flow cytometry and living cells (FITC$^-$/PI$^-$), necrotic cells (FITC$^+$/PI$^+$), and apoptotic cells (FITC$^+$/PI$^-$) were quantified. The proportions of apoptotic cells in the control, 20, and 40 µg treatment groups were 8.87%, 22.3%, and 45.11%, respectively ($p < 0.01$) (Fig. 7). These results revealed that NK-92 Exo can trigger apoptosis in B16F10/effluc cells *in vitro*.

To confirm the cell death mechanism, we also assessed apoptosis-related proteins by western blot analysis. As shown in the schematic diagram (Fig. 8A) of the apoptosis signaling pathway induced by the NK cells, we examined the levels of caspase-3, cleaved caspase-3, cleaved PARP, and cytochrome-c proteins. The abundances of cleaved caspase-3, cleaved PARP, and cytochrome-c increased by 3.78-fold, 1.32-fold, and 1.66-fold, respectively, after 24 h NK-92 Exo treatment (Fig. 8B). These results indicated that NK-92 Exo could induce the apoptosis of the cancer cells by both the extrinsic and intrinsic apoptotic pathways.

To understand the mechanistic pathways of cell death related to NK-92 Exo, we assessed the abundances of the MAPK signaling proteins p-ERK and p38. The abundance of the proliferation signaling molecule p-ERK was decreased to 28% of that in the control by NK-92 Exo treatment (Supplementary Fig. 4A). To confirm that NK-92 Exo can affect the MAPK signaling pathways, we also quantified p38 protein. After 24 h treatment with NK-92 Exo, the level of p38 protein increased by 4.71-fold (Supplementary Fig. 4B), suggesting that NK-92 Exo can inhibit the proliferation of these cancer cells.

Quantification of TNF-α

We performed ELISA to confirm the presence of the cytokine TNF-α in NK-92 Exo. The results indicated that the NK cells, culture medium, and NK-92 Exo all contained TNF-α (Supplementary Fig. 4C).

Effect of NK-92 Exo on melanoma xenograft assessed by *in vivo* BLI

A schematic diagram of the *in vivo* experiments is presented in Supplementary Fig. 5. Twelve mice were used in this experiment. Tumor cells were subcutaneously injected and the mice were divided

into two groups randomly at day 7 ($n = 6$ per group). We administered 20 µg NK-92 Exo and PBS intratumorally to the treatment and control groups, respectively. The intensity of the bioluminescence signals from the tumors in the two groups did not show obvious differences on the first day after treatment. From days 2–5, the signal intensity of the NK-92 Exo treatment group was significantly lower than that of the control group ($p < 0.05$, Figs. 9A and B). After harvesting the tumors from the mice, *ex vivo* experiments were performed. The masses of tumors in the NK-92 Exo treatment group were lower than those of tumors in the control group ($p < 0.001$) (Fig. 10C). *Ex vivo* BLI of the tumors showed similar results to *in vivo* BLI; the control group exhibited an almost 3.5-fold increase in signal intensity compared with the NK-92 Exo treatment group (Figs. 9C and D).
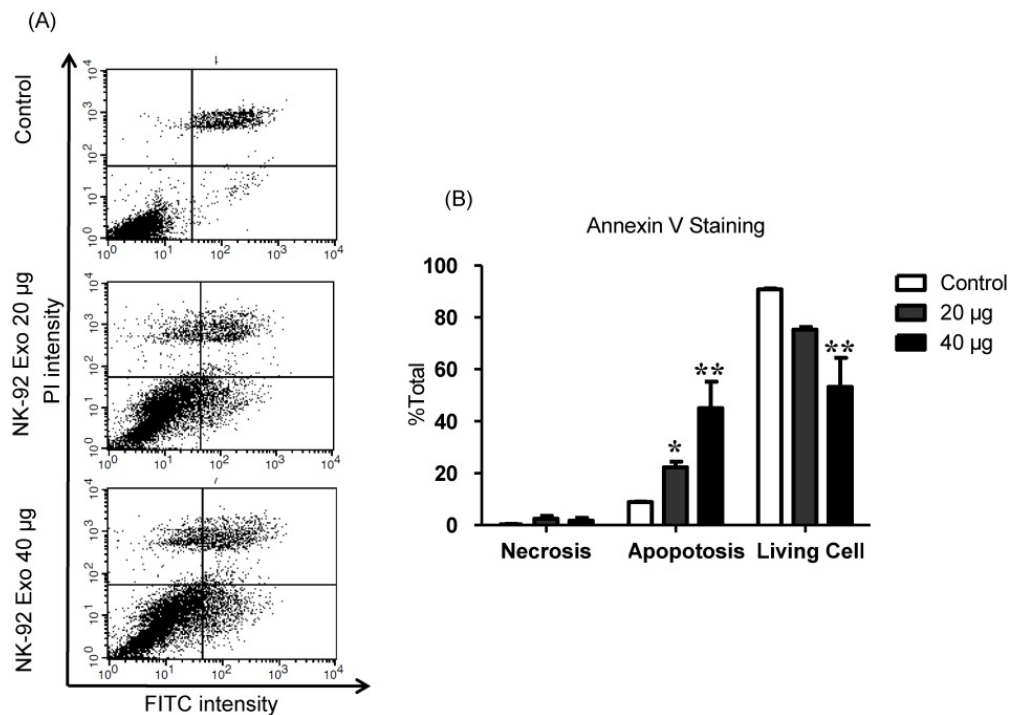

Fig 7. NK-92 Exo induced apoptosis in melanoma cancer cells *in vitro*. (A) The apoptosis of B16F10/effluc cells induced by NK-92 Exo was assessed by flow cytometric analysis using Annexin V. (B) Quantitation of the scatter plots. The apoptotic rate of B16F10/effluc cells was significantly increased by NK-92 Exo. Experiments were performed in triplicate and mean values ± SD were plotted. *$p < 0.05$, **$p < 0.01$.
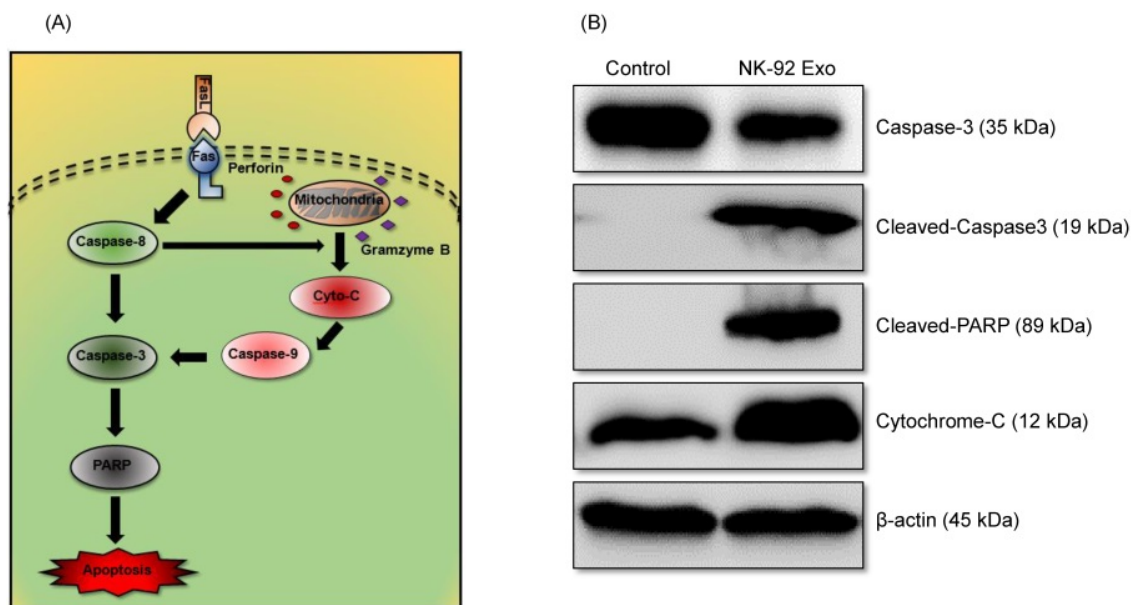

Fig 8. Mechanism of the apoptotic induction in B16F10/effluc cells by NK-92 Exo. (A) Diagram of the apoptosis signaling pathway by NK-92 Exo. (B) Western blot analysis of important proteins in the apoptosis signaling pathway. With NK-92 Exo treatment, the abundances of cleaved caspase-3, cleaved PARP, and cytochrome c increased by 3.78-fold 3.49-fold, and 1.66-fold, respectively.
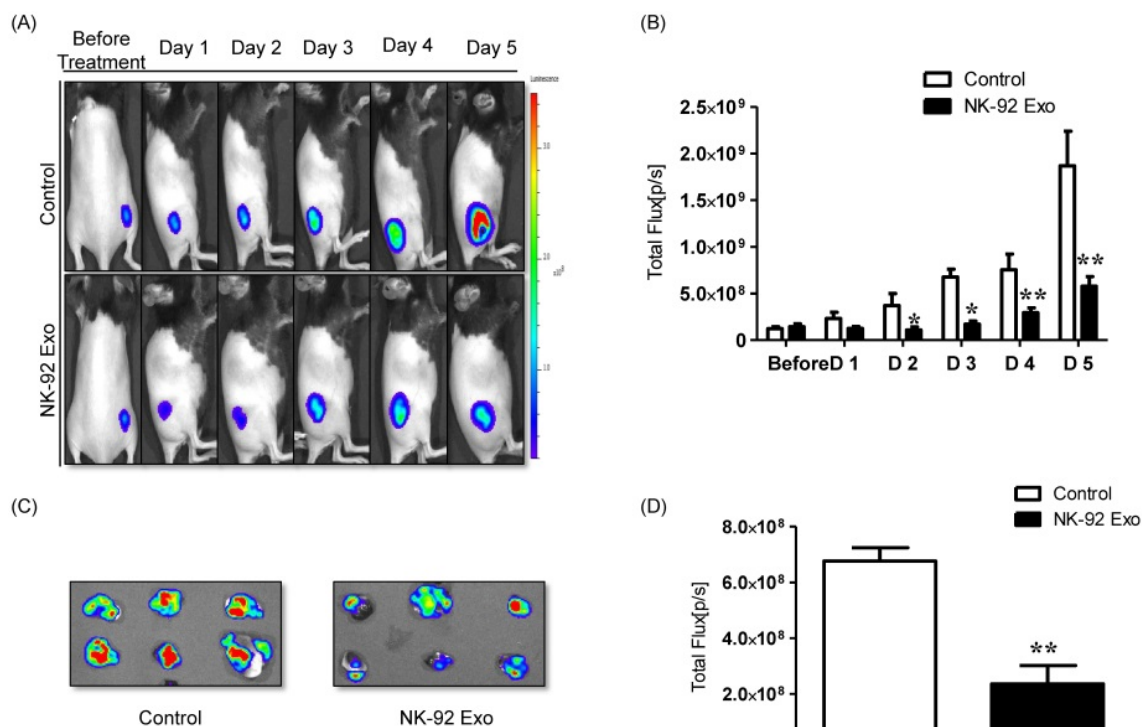
Fig 9. Anti-tumor effect of NK-92 Exo on melanoma cancer cells *in vivo* and *ex vivo*. (A) BLI measurements of the B16F10/effluc activity in mice were performed in the control and treatment groups. In the treatment group, 20 µg of NK-92 Exo was injected into tumors twice. (B) Quantitative BLI of B16F10/effluc activity. (C) BLI of the *ex vivo* tumor activity. (D) Quantitative BLI of *ex vivo* B16F10/effluc activity. Values are expressed as the mean ± SD, $*p < 0.05$ $**p < 0.01$.
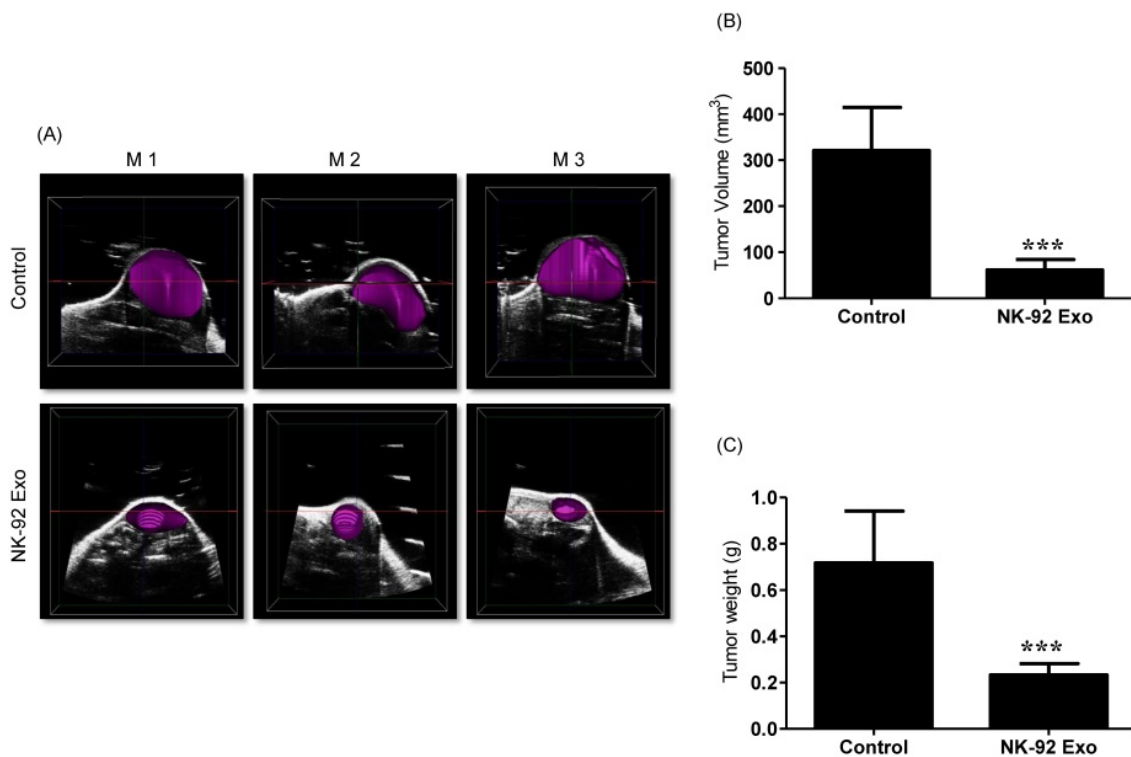

Fig 10. Ultrasound imaging of tumors *in vivo*. After collecting the B model imaging of (A), the tumor was imaged by ultrasonography. (B) Tumor volumes were measured by 3-D imaging obtained using software. (C) Tumor masses (g) were measured after mice were sacrificed. Values are expressed as the mean ± SD, $***p < 0.001$.

3-D tumor model reproduction and *in vivo* tumor measurement

Previous studies have reported that ultrasound imaging can provide reliable tumor volume estimates in animal tumor studies [21, 22]. To confirm that the BLI results were related to tumor growth, we also performed ultrasound imaging. First, we collected tumor B model images using the ultrasound imaging system; then, we reproduced the 3-D pattern. In the quantitative analysis, the average tumor volume of the NK-92 Exo treatment group was less than 100 mm^3, but that of the control group was more than 300 mm^3 ($p < 0.001$, Figs. 10A and B). These results supported the reliability of the BLI results and demonstrated the immunotherapeutic capacity of the NK-92 Exo.

Discussion

In this study, we successfully isolated exosomes from NK cells and showed that they contained immunologically active components of those cells. We also demonstrated that NK-92 Exo exert cytotoxic activity against tumor cells. To our knowledge, this is the first report to demonstrate an antitumor effect of NK exosomes *in vivo*.

NK cells are an important part of the innate immune system, based on their ability to lyse infected cells without sensitization [23]. They are also able to produce cytokines and growth factors that affect other immune system components such as dendritic cells, neutrophils, and T lymphocytes. Exosomes are 30–150-nm spherical vesicles that are secreted by almost all cells and deliver several molecules including proteins, lipids, and nucleic acids to target cells [24, 25]. Thus, NK-derived exosomes may be suitable as a novel approach for immunotherapy against cancer cells. To explore the function of NK-92 Exo, we first isolated them from NK cell culture medium using both normal ultracentrifugation and density gradient ultracentrifugation, then confirmed their morphology and size by TEM (Fig. 1). Characterization of NK-92 Exo revealed that NK-92 Exo were 100–150 nm in size with a complete membrane structure and displayed CD63, which has been regarded as an exosome marker in previous studies [15, 20, 26]. Perforin is considered to be the core molecule required for NK cell-mediated tumor killing by inducing the apoptosis of target cells [27-29], and death-receptor pathways (involving FasL and TRAIL) can also be engaged [30]. In this study, we confirmed by western blot analysis that NK-92 Exo contain perforin and FasL proteins (Fig. 2). Notably, the abundances of FasL and perforin were higher in NK-92 Exo than those in NK cells (Fig. 2). Clinical outcomes have shown that approximately 71.4% of patients harbor metastatic melanoma that is resistant to immunotherapy [31]. Here, we have demonstrated that exosomes from NK cells exert an antitumor effect on aggressive melanoma cells, as measured by BLI and cell proliferation assays using B16F10/effluc cells as a model system (Figs. 3 and 4). After 24 h co-incubation, the BLI signal of the NK-92 Exo group was significantly diminished compared with a vehicle-treated control group. Although an earlier study reported that high doses of NK exosomes could inhibit cancer growth [32], we proved in this study that even low concentrations of NK-92 Exo could have an antitumor effect. In the current study, we also demonstrated that NK-92 Exo displayed a significant cytotoxic effect on other human cancer cell lines. Like melanomas, 92% of gastric carcinomas also show immunotherapy resistance [33]. However, NK-92 Exo exerted a therapeutic effect on human colon and gastric cancer cells (Supplementary Fig. 6). To measure the possible side effects of NK-92 Exo on healthy human cells, cytotoxicity was ascertained by BLI and CCK-8 assays using a human kidney cell line. Based on the results, NK-92 Exo did not display significant cytotoxicity against normal cells even after 24 h co-culture (Fig. 4B and Supplementary Fig. 3B). Taken together, NK-92 Exo could be a promising candidate for use in the immunotherapy of solid tumors.

It has been proposed that apoptosis is an important mechanism in NK cell-based immunotherapy [34]. Perforin triggers the intrinsic pathway and elevates the release of cytochrome-c [27, 29]. FasL triggers the extrinsic apoptotic pathway by activating caspase-8, caspase-3, and PARP [30]. In the current study, we found that NK exosomes exert their antitumor effect because of the presence of both perforin and FasL (Fig. 2). This corroborates with the results of the western blot analysis, where the abundances of cleaved caspase-3, cleaved PARP, and cytochrome-c proteins all increased in the NK-92 Exo treatment group (Fig. 8B), representing the antitumor effect of NK-92 Exo mediated via both the extrinsic and intrinsic apoptosis pathways. Previous studies have demonstrated that NK cells can release exosomes in both resting and activated conditions, and even resting NK-derived exosomes contain both FasL and perforin [24, 32]. Therefore, compared with the complex procedure of collecting NK cells from PBMCs followed by activation for 7 days, NK-92 Exo can be feasibly and rapidly isolated and used in clinics for immunotherapy.

We further analyzed signaling molecules involved in cellular proliferation. A high level of ERK activation is linked to early metastasis and a short

survival time [35]. In the current study, we demonstrated the downregulation of p-ERK protein, which has a close relationship with decreased cell growth, after NK-92 Exo treatment (Supplementary Fig. 4A). Previously, Kalimuthu *et al.* reported that extracellular vesicles derived from mesenchymal stem cells achieve their antitumor effect through the MAPK signaling pathways [15]. To confirm NK-92 Exo participation in the MAPK pathways and its influence on melanoma cell proliferation, we investigated other proteins involved in the three main MAPK pathways. It has been demonstrated that the p38 pathway exerts a tumor suppressor function by negatively regulating cell survival and proliferation. In mammalian cells, p38 is strongly activated by multiple factors, including ultraviolet light, cytokines, and hypoxia [36]. Our results clearly indicate that, after 24 h treatment with NK-92 Exo, p38 protein levels were elevated by 4.71-fold (Supplementary Fig. 4B). We believe that the therapeutic effect of NK-92 Exo may be related to TNF-α (Supplementary Fig. 4D). TNF-α, known to be a major pro-inflammatory cytokine, was shown to be contained in exosomes derived from various immune cells, such as DCs or macrophages, and this protein produced various biological effects on interacting cells [26, 37, 38]. This is the first demonstration that NK cell exosomes contain TNF-α, and confirms that TNF-α impacts melanoma cell proliferation, survival, and apoptosis. Our results further suggest that NK-92 Exo-mediated melanoma cytotoxicity is related to their contents of FasL and TNF-α.

In the current study, we used melanoma xenograft implantation animal models, and the NK-92 Exo were administered by intratumoral injection. Optical imaging by fluorescence, bioluminescent techniques, or radionuclide visualization by PET is commonly used in animal models [6, 39-41]. For the evaluation of the therapeutic effect of NK-92 Exo in a living animal model, we established a stable cell line equipped with a reporter gene. The results demonstrated that NK-92 Exo could inhibit tumor growth. In 1998, using animal models, Zitvogel *et al.* proposed that DC-derived exosomes promote T-cell antitumor immune responses, and other subsequent experiments have established the successful application of immune cell exosomes in animal tumor models [15, 25, 26, 42-44]. Although the immune surveillance properties of NK-92 Exo have been proven *in vitro* [32], an *in vivo* immunotherapeutic effect had not been clearly proven. In the current study, NK-92 Exo inhibited tumor growth ($p < 0.01$) and reduced tumor volume ($p < 0.001$) compared with the control group (Figs. 9 and 10). Taken together, the *in vivo* experiments revealed an obvious antitumor effect of NK-92 Exo.

The complexities of the tumor microenvironment influence the effects of immune cell therapy for cancerous diseases and can decrease the effectiveness of NK cell-based immunotherapy. It has been well documented that acidity around tumors can reduce the release of perforin/granzymes from NK cells and inhibit Fas/FasL interaction [40, 45, 46]. However, acidity favors the accumulation and delivery of exosomes, because the low pH attracts them and promotes membrane fusion [47]. Therefore, NK-92 Exo immunotherapy may have advantages over whole NK cell-based therapy.

The predominant method of NK cell-based immunotherapy is the transfer of unmodified autologous or allogeneic NK cells [27]. Unlike DC and cytokine-induced killer cell therapies, NK cells can be used from not only autologous sources, but also allogeneic ones; this provides more clinical applications for NK-92 Exo. However, although treatment with enriched autologous NK cells has been employed more frequently as a cancer therapy in recent years, no success of this approach against metastatic melanoma, renal cell carcinoma, or advanced gastrointestinal cancer has been identified [48, 49]. Moreover, allogeneic NK cells have been utilized owing to the limitations of the lack of donors and restricted blood types; immunotherapy is difficult for large-scale and long-term use in patients [49, 50]. Conversely, treatment with NK-92 Exo has significant advantages. Compared with the harvesting of NK cells from PBMCs, the generation of NK-92 Exo from NK cell medium has been well established and is a relatively simple process that requires only minimal laboratory effort and reagents [32]. Furthermore, evidence has shown that MHC class I presentation by exosomes is less than that by NK cells, which may elicit diminished immune rejection, and they can thus be incorporated with many other personalized treatments [6, 51]. Therefore, NK-92 Exo may represent a valuable and reliable therapeutic option, as these can be obtained from any donor and could be useful for treating human cancers.

Conclusion

The results of the current study suggest that exosomes derived from NK cells exert cytotoxic effects on melanoma cells and thus warrant further development as a potential immunotherapeutic strategy for cancer.

Supplementary Material

Supplementary figures.
http://www.thno.org/v07p2732s1.pdf

Acknowledgments

Competing Interests

The authors have declared that no competing interest exists.

References

1. Garbe C, Eigentler TK, Keilholz U, Hauschild A, Kirkwood JM. Systematic review of medical treatment in melanoma: current status and future prospects. Oncologist. 2011; 16: 5-24.
2. Chin L, Garraway LA, Fisher DE. Malignant melanoma: genetics and therapeutics in the genomic era. Genes Dev. 2006; 20: 2149-82.
3. Franklin C, Livingstone E, Roesch A, Schilling B, Schadendorf D. Immunotherapy in melanoma: Recent advances and future directions. European journal of surgical oncology : Eur J Surg Oncol. 2017; 43: 604-11.
4. Shimasaki N, Coustan-Smith E, Kamiya T, Campana D. Expanded and armed natural killer cells for cancer treatment. Cytotherapy. 2016; 18: 1422-34.
5. Ruggeri L, Capanni M, Urbani E, Perruccio K, Shlomchik WD, Tosti A, et al. Effectiveness of donor natural killer cell alloreactivity in mismatched hematopoietic transplants. Science. 2002; 295: 2097-100.
6. Chen X, Han J, Chu J, Zhang L, Zhang J, Chen C, et al. A combinational therapy of EGFR-CAR NK cells and oncolytic herpes simplex virus 1 for breast cancer brain metastases. Oncotarget. 2016; 7: 27764-77.
7. Balsamo M, Pietra G, Vermi W, Moretta L, Mingari MC, Vitale M. Melanoma immunoediting by NK cells. Oncoimmunology. 2012; 1: 1607-9.
8. Sconocchia G, Arriga R, Tornillo L, Terracciano L, Ferrone S, Spagnoli GC. Melanoma cells inhibit NK cell functions. Cancer Res. 2012; 72: 5428-9; author reply 30.
9. Staals RH, Pruijn GJ. The human exosome and disease. Adv Exp Med Biol. 2011; 702: 132-42.
10. Peinado H, Aleckovic M, Lavotshkin S, Matei I, Costa-Silva B, Moreno-Bueno G, et al. Melanoma exosomes educate bone marrow progenitor cells toward a pro-metastatic phenotype through MET. Nat Med. 2012; 18: 883-91.
11. Andreola G, Rivoltini L, Castelli C, Huber V, Perego P, Deho P, et al. Induction of lymphocyte apoptosis by tumor cell secretion of FasL-bearing microvesicles. J Exp Med. 2002; 195: 1303-16.
12. Danesh A, Inglis HC, Jackman RP, Wu S, Deng X, Muench MO, et al. Exosomes from red blood cell units bind to monocytes and induce proinflammatory cytokines, boosting T-cell responses in vitro. Blood. 2014; 123: 687-96.
13. Chaput N, Taieb J, Schartz N, Flament C, Novault S, Andre F, et al. The potential of exosomes in immunotherapy of cancer. Blood Cells Mol Dis. 2005; 35: 111-5.
14. Pitt JM, Andre F, Amigorena S, Soria JC, Eggermont A, Kroemer G, et al. Dendritic cell-derived exosomes for cancer therapy. J Clin Invest . 2016; 126: 1224-32.
15. Kalimuthu S, Gangadaran P, Li XJ, Oh JM, Lee HW, Jeong SY, et al. In Vivo therapeutic potential of mesenchymal stem cell-derived extracellular vesicles with optical imaging reporter in tumor mice model. Sci Rep. 2016; 6: 30418.
16. Banchereau J, Steinman RM. Dendritic cells and the control of immunity. Nature. 1998; 392: 245-52.
17. Palucka K, Banchereau J. Cancer immunotherapy via dendritic cells. Nat Rev Cancer. 2012; 12: 265-77.
18. Klinker MW, Lizzio V, Reed TJ, Fox DA, Lundy SK. Human B Cell-Derived Lymphoblastoid Cell Lines Constitutively Produce Fas Ligand and Secrete MHCII(+)FasL(+) Killer Exosomes. Front Immunol. 2014; 5: 144.
19. Thery C, Amigorena S, Raposo G, Clayton A. Isolation and characterization of exosomes from cell culture supernatants and biological fluids. Curr Protoc Cell Biol. 2006; Chapter 3: Unit 3 22.
20. Lee JK, Park SR, Jung BK, Jeon YK, Lee YS, Kim MK, et al. Exosomes derived from mesenchymal stem cells suppress angiogenesis by down-regulating VEGF expression in breast cancer cells. PLoS One. 2013; 8: e84256.
21. Cheung AM, Brown AS, Hastie LA, Cucevic V, Roy M, Lacefield JC, et al. Three-dimensional ultrasound biomicroscopy for xenograft growth analysis. Ultrasound Med Biol. 2005; 31: 865-70.
22. Wirtzfeld LA, Wu G, Bygrave M, Yamasaki Y, Sakai H, Moussa M, et al. A new three-dimensional ultrasound microimaging technology for preclinical studies using a transgenic prostate cancer mouse model. Cancer Res. 2005; 65: 6337-45.
23. Hellstrom I, Hellstrom KE. Cytotoxic effect of lymphocytes from pregnant mice on cultivated tumor cells. I. Specificity, nature of effector cells and blocking by serum. Int J Cancer. 1975; 15: 1-16.
24. Fais S. NK cell-released exosomes: Natural nanobullets against tumors. Oncoimmunology. 2013; 2: e22337.
25. Katakowski M, Buller B, Zheng X, Lu Y, Rogers T, Osobamiro O, et al. Exosomes from marrow stromal cells expressing miR-146b inhibit glioma growth. Cancer Lett. 2013; 335: 201-4.
26. Gao W, Liu H, Yuan J, Wu C, Huang D, Ma Y, et al. Exosomes derived from mature dendritic cells increase endothelial inflammation and atherosclerosis via membrane TNF-alpha mediated NF-kappaB pathway. J Cell Mol Med. 2016; 20: 2318-2327.
27. Guillerey C, Huntington ND, Smyth MJ. Targeting natural killer cells in cancer immunotherapy. Nat Immunol. 2016; 17: 1025-36.
28. Brodbeck T, Nehmann N, Bethge A, Wedemann G, Schumacher U. Perforin-dependent direct cytotoxicity in natural killer cells induces considerable knockdown of spontaneous lung metastases and computer modelling-proven tumor cell dormancy in a HT29 human colon cancer xenograft mouse model. Mol Cancer. 2014; 13: 244.
29. Trapani JA, Smyth MJ. Functional significance of the perforin/granzyme cell death pathway. Nat Rev Immunol. 2002; 2: 735-47.
30. Augstein P, Heinke P, Schober C, Salzsieder E. Impact of cytokine- and FasL-induced apoptosis in the beta-cell line NIT-1. Horm Metab Res. 2009; 41: 207-12.
31. Erdag G, Schaefer JT, Smolkin ME, Deacon DH, Shea SM, Dengel LT, et al. Immunotype and immunohistologic characteristics of tumor-infiltrating immune cells are associated with clinical outcome in metastatic melanoma. Cancer Res. 2012; 72: 1070-80.
32. Lugini L, Cecchetti S, Huber V, Luciani F, Macchia G, Spadaro F, et al. Immune surveillance properties of human NK cell-derived exosomes. J Immunol. 2012; 189: 2833-42.
33. Oba J, Nakahara T, Abe T, Hagihara A, Moroi Y, Furue M. Expression of c-Kit, p-ERK and cyclin D1 in malignant melanoma: an immunohistochemical study and analysis of prognostic value. J Dermatol Sci. 2011; 62: 116-23.
34. Lee HW, Singh TD, Lee SW, Ha JH, Rehemtulla A, Ahn BC, et al. Evaluation of therapeutic effects of natural killer (NK) cell-based immunotherapy in mice using in vivo apoptosis bioimaging with a caspase-3 sensor. FASEB J. 2014; 28: 2932-41.
35. Satyamoorthy K, Li G, Gerrero MR, Brose MS, Volpe P, Weber BL, et al. Constitutive mitogen-activated protein kinase activation in melanoma is mediated by both BRAF mutations and autocrine growth factor stimulation. Cancer Res. 2003; 63: 756-9.
36. Cargnello M, Roux PP. Activation and function of the MAPKs and their substrates, the MAPK-activated protein kinases. Microbiol Mol Biol Rev. 2011; 75: 50-83.
37. McDonald MK, Tian Y, Qureshi RA, Gormley M, Ertel A, Gao R, et al. Functional significance of macrophage-derived exosomes in inflammation and pain. Pain. 2014; 155: 1527-39.
38. Bretz NP, Ridinger J, Rupp AK, Rimbach K, Keller S, Rupp C, et al. Body fluid exosomes promote secretion of inflammatory cytokines in monocytic cells via Toll-like receptor signaling. J Biol Chem. 2013; 288: 36691-702.
39. Adumeau P, Carnazza KE, Brand C, Carlin SD, Reiner T, Agnew BJ, et al. A Pretargeted Approach for the Multimodal PET/NIRF Imaging of Colorectal Cancer. Theranostics. 2016; 6: 2267-77.
40. Kruschinski A, Moosmann A, Poschke I, Norell H, Chmielewski M, Seliger B, et al. Engineering antigen-specific primary human NK cells against HER-2 positive carcinomas. Proc Natl Acad Sci USA. 2008; 105: 17481-6.
41. Kim JE, Kalimuthu S, Ahn BC. In vivo cell tracking with bioluminescence imaging. Nucl Med Mol Imaging. 2015; 49: 3-10.
42. Zitvogel L, Regnault A, Lozier A, Wolfers J, Flament C, Tenza D, et al. Eradication of established murine tumors using a novel cell-free vaccine: dendritic cell-derived exosomes. Nat Med. 1998; 4: 594-600.
43. Damo M, Wilson DS, Simeoni E, Hubbell JA. TLR-3 stimulation improves anti-tumor immunity elicited by dendritic cell exosome-based vaccines in a murine model of melanoma. Sci Rep. 2015; 5: 17622.
44. Kim SH, Bianco N, Menon R, Lechman ER, Shufesky WJ, Morelli AE, et al. Exosomes derived from genetically modified DC expressing FasL are anti-inflammatory and immunosuppressive. Mol Ther. 2006; 13: 289-300.

45. Baginska J, Viry E, Paggetti J, Medves S, Berchem G, Moussay E, et al. The critical role of the tumor microenvironment in shaping natural killer cell-mediated anti-tumor immunity. Front Immunol. 2013; 4: 490.

46. Ames E, Hallett WH, Murphy WJ. Sensitization of human breast cancer cells to natural killer cell-mediated cytotoxicity by proteasome inhibition. Clin Exp Immunol. 2009; 155: 504-13.

47. Parolini I, Federici C, Raggi C, Lugini L, Palleschi S, De Milito A, et al. Microenvironmental pH is a key factor for exosome traffic in tumor cells. J Biol Chem. 2009; 284: 34211-22.

48. Parkhurst MR, Riley JP, Dudley ME, Rosenberg SA. Adoptive transfer of autologous natural killer cells leads to high levels of circulating natural killer cells but does not mediate tumor regression. Clin Cancer Res. 2011; 17: 6287-97.

49. Klingemann H, Boissel L, Toneguzzo F. Natural Killer Cells for Immunotherapy - Advantages of the NK-92 Cell Line over Blood NK Cells. Front Immunol. 2016; 7: 91.

50. Shah NN, Baird K, Delbrook CP, Fleisher TA, Kohler ME, Rampertaap S, et al. Acute GVHD in patients receiving IL-15/4-1BBL activated NK cells following T-cell-depleted stem cell transplantation. Blood. 2015; 125: 784-92.

51. Muller N, Michen S, Tietze S, Topfer K, Schulte A, Lamszus K, et al. Engineering NK Cells Modified With an EGFRvIII-specific Chimeric Antigen Receptor to Overexpress CXCR4 Improves Immunotherapy of CXCL12/SDF-1alpha-secreting Glioblastoma. J Immunother. 2015; 38: 197-210.